Food and Chemical Toxicology 133 (2019) 110766

Contents lists available at ScienceDirect

Food and Chemical Toxicology

journal homepage: www.elsevier.com/locate/foodchemtox

Obesity associated with coal ash inhalation triggers systemic inflammation and oxidative damage in the hippocampus of rats

Juciano Gasparotto[a,b,*], Paloma Rodrigues Chaves[a], Katia da Boit Martinello[b], Luis Felipe Silva Oliveira[b], Daniel Pens Gelain[a], José Claudio Fonseca Moreira[a]

[a] Centro de Estudos Em Estresse Oxidativo, Departamento de Bioquímica, Instituto de Ciências Básicas da Saúde, Universidade Federal Do Rio Grande Do Sul, Porto Alegre, RS, Brazil

[b] Departamento de Civil y Ambiental, Universidad de la Costa, Calle 58 #55-66, CP 080002, Barranquilla, Atlántico, Colombia

ARTICLE INFO

Keywords:
Obesogenic diet
Air pollution
Hippocampus
Oxidative damage
Inflammation

ABSTRACT

People with large amounts of adipose tissue are more vulnerable and more likely to develop diseases where oxidative stress and inflammation play a pivotal role, than persons with a healthy weight. Atmospheric contamination is a reality to which a large part of the worldwide population is exposed. Half of today's global electrical energy is derived from coal. Each organism, in its complexity, responds in different ways to dietary compounds and air pollution. The objective of this study was to investigate the effects of obesity and coal ash inhalation within the parameters of oxidative damage and inflammation in different regions of the brain of rats. A diet containing high-fat concentration was administered chronically to rats, along with exposure to coal ash, simulating the contamination that occurs daily throughout human life. High-resolution transmission electron microscopy was performed to identify the particles present in coal ash samples. Our results demonstrated that obese rats exposed to coal ash inhalation were more affected by oxidative damage with subsequent systemic inflammation in the hippocampus. Since there is an inflammatory predisposition caused by obesity, the inhalation of nanoparticles increases the levels of free radicals, resulting in systemic inflammation and oxidative damage, which can lead to chronic neurodegeneration.

1. Introduction

In this study, we investigate the effects of the association between obesity and exposure to coal ash particles in different rat brain regions. Obesity is characterized by an exacerbated increase in body fat, which in turn acts as an endocrine organ, producing and releasing a series of hormones and molecules that affect the physiology and biochemistry of organisms (Bluher, 2019; Siino et al., 2018).

Obesity represents a significant health challenge since it substantially increases the risk of diseases such as type 2 diabetes mellitus, fatty liver disease, stroke and dementia (Bluher, 2019), and recently obesity is seen as a risk factor for Alzheimer's disease due to constant hyperglycemia (Alford et al., 2018; Xue and Ideraabdullah, 2016).

In order to induce obesity in animals, we used a chronic obesogenic diet for 6 months. The diet consisted of 60% fat and was validated by checking the exponential increase of the animal's weight.

Obese and non-obese animals were exposed to an environment polluted by coal ash. Air pollution is the fifth largest mortality risk factor worldwide (HEI, 2019). More than 90% of the world's population lives in areas exceeding the WHO Guideline for healthy air. More than half live in areas that do not even meet the WHO's least-stringent air quality target (HEI, 2019).

Coal generates almost half of the global energy around the world, notably used by industrial plants and factories. According to the World Health Organization (WHO, 2018), 97% of cities in low- and middle-income countries with more than 100,000 inhabitants do not meet WHO air quality guidelines.

Good quality air is vital for the correct functioning of an organism. It has been proven that the emission of a number of pollutants released by factories etc reaches their surrounding neighborhood, causing a public concern over possible adverse health effects for the population (Rovira et al., 2019). Even cases of short period exposure to elevated concentrations during commuting between home and school are associated with adverse impacts on cognitive development in schoolchildren (Alvarez-Pedrerol et al., 2017). Among these alterations, memory impairment was identified, which is directly related to the region affected in our study.

In our experiments, the animals were exposed to coal ash particles

* Corresponding author. Rua Ramiro Barcelos, 2600 – Anexo, CEP 90035-003, Porto Alegre, RS, Brazil.
E-mail address: Juciano.gasparotto@gmail.com (J. Gasparotto).

https://doi.org/10.1016/j.fct.2019.110766
Received 12 July 2019; Received in revised form 12 August 2019; Accepted 16 August 2019
Available online 17 August 2019
0278-6915/

collected as a result of the burning process. We designed a particle propellant chamber to simulate atmospheric contamination which controlled the volume of coal ash and the animal's exposure time (Gasparotto et al., 2018).

Obese people are more susceptible to air pollution-associated cardiovascular disease and respiratory disorders (Gasparotto et al., 2018; McCormack et al., 2015). However, few studies investigate the relationship between obesity and environmental contamination on the central nervous system.

The present work aimed to investigate the effects of obesity and exposure to intensely coal ash polluted air on the prefrontal cortex, striatum, hippocampus, cerebellum, and serum of rats with high fat diet. Weight and glycemia were monitored. The current study investigated parameters of oxidative damage and pro-inflammatory cytokines in rats, while high-resolution transmission electron microscopy was performed to study the compounds present in coal ash.

2. Materials and methods

2.1. Chemicals

The chemicals used in the study were as follows: Catalase (CAT, EC 1.11.1.6), superoxide dismutase (SOD, EC 1.15.1.1), hydrogen peroxide (H_2O_2), epinephrine, nicotinamide adenine dinucleotide phosphate (NADPH), thiobarbituric acid (TBA), and Ethylenediaminetetraacetic acid (EDTA), purchased from Merck (Massachusetts, EUA). Tumor necrosis factor-a (TNF-α, ab6671) and Interleukin-1b (IL-1β, ab9722) antibodies were purchased from Abcam® (Cambridge, UK). Secondary antibody anti-Rabbit IgG, peroxidase conjugate (#AP132P) was purchased from Merck (Massachusetts, EUA). ELISA microplates and TMB spectrophotometric detection kit were from Greiner Bio-One (Monroe, USA) and BD Biosciences (San Diego, USA) respectively.

For further information and requests for reagents, please contact juciano.gasparotto@gmail.com.

2.2. Data reporting

We conducted all procedures presented in this study according to the animal research guidelines from NIH, the animal care standards of the Committee of Ethics for the Use of Animals (CEUA) of the Federal University of Rio Grande do Sul (UFRGS) and the Guide for the Care and Use of Laboratory Animals (2011).

2.3. Animals

A total of 32 adult male Wistar rats were used. The rats were housed under a 12hr light/dark cycle. At the time of the experiments, animals were 60 days old. The animals were obtained from our breeding colony and used in scientific experiments for the first time. All animals were healthy. Animals had free access (*ad libitum)* to water. Access to food was controlled.

2.4. Experimental model

Animals were randomly assigned numbers and separated into two groups ($n = 16$ per group). Diets were administered for 5 months as follows:

Group 1 (control): Commercial food (Chow Nuvilab CR-1 type; Curitiba, PR, Brazil).

Group 2: High-fat diet (HFD), containing 60% fat, composed of 59% lard and 1% soybean oil, 20% protein, 15% carbohydrates and 5% mineral salts (de Assis et al., 2009).

After 5 months of diet administration, the animals were divided into four groups:

a) Control unexposed to coal ash Inhalation and non-obese (control $n = 8$);
b) Coal ash inhalation ($n = 8$);
c) HFD unexposed to coal ash Inhalation (HFD, $n = 8$);
d) HFD + coal ash Inhalation ($n = 8$).

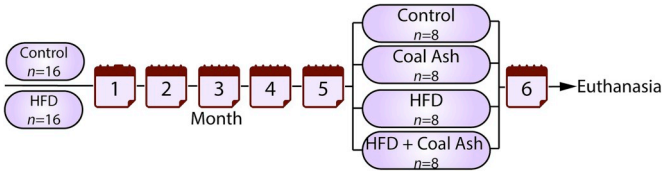

Fig. 1. Timeline. Description of the protocol used for diet and exposure to coal ash.

During the exposure time to coal ash (1 month), the diets were maintained, totaling six months of treatment. The food intake was monitored daily. For more details see Fig. 1.

2.5. Rats exposed to coal ash particle inhalation

Wistar rats were submitted to a coal ash inhalation protocol (Gasparotto et al., 2018) during which each rat entered bodily into a 21 L glass inhalation chamber. Eight rats of each group were allocated to the glass chamber and exposed to coal ash inhalation (10 mg/m^3) for 3 h per day totaling 30 days of coal ash circulation. The concentrations were continuously recorded using a 25 mm filter (Intox Products, USA).

A particle propeller chamber is a realistic tool for studying occupational hazards. This chamber, which simulates environmental contamination, was designed and built by our research group (Supplementary Fig. 1). In it, animals are exposed to conditions very similar to the environmental contamination generated by burning coal. It is therefore possible to control the amount of emitted coal ash and monitor the effects of exposure in vivo.

2.6. Tissue samples

The animals were euthanized using a guillotine, 24 h after the last inhalation. Serum and brain were analyzed. The blood was centrifuged at 2000 RPM for 15 min to separate the serum. We investigated four brain regions: the prefrontal cortex, the hippocampus, the striatum, and the cerebellum.

For accuracy and reproducible results, the structures were isolated using the Rodent Brain Matrix (RBM-4000C - ASI instruments, Michigan, USA) and rat brain atlas (Paxinos and Watson, 2007). The tissue samples were stored at −20 °C.

2.7. Enzymatic activity

To perform the enzymatic activities, prefrontal cortex, hippocampus, striatum, and cerebellum were homogenized in 50 mm of phosphate buffer ($KH_2PO_4$and K_2HPO_4, pH 7.4) with a homogenizer (Cole-Parmer's - EW-04727-02, IL, USA) and centrifuged (2000 × *g* for 10 min). Supernatants were isolated and total protein content was quantified by Bradford assay (Bradford, 1976), and normalized to 1 μg protein/μL.

a) Catalase - CAT activity was evaluated measuring the rate of hydrogen peroxide (H_2O_2) decomposition in a spectrophotometer at 240 nm. Bubble formation from oxygen generation by CAT activity did not interfere with the measurement of these activities in the linear range used to measure them. CAT activity is expressed as units per milligram of protein (Aebi, 1984).
b) Superoxide dismutase - SOD activity was evaluated by quantifying the inhibition of superoxide-dependent epinephrine auto-oxidation. The reaction was induced by the addition of adrenaline 2 mm,

generating superoxide. The adrenochrome formation was monitored at 480 nm for 5 min (32 °C) in a spectrophotometer. Results were expressed as SOD units per milligram of protein (Misra and Fridovich, 1972).

c) Glutathione peroxidase - GPx activity was evaluated by monitoring the rate of NADPH oxidation using tert-butyl hydroperoxide, reduced glutathione (GSH), and glutathione reductase. The reaction was monitored in a spectrophotometer at 340 nm for 6 min (37 °C). Results were expressed as GPx units per milligram of protein (Wendel, 1981).

d) Glutathione S-transferases - GST activity was evaluated measuring the formation of conjugated GSH (glutathione) and 1-Chloro-2,4-dinitrobenzene (CDNB). The reaction was monitored in a spectrophotometer at 340 nm for 10 min (37 °C). Results were expressed as GST units per milligram of protein (Habig et al., 1974).

2.8. Oxidative damage

a) Lipid peroxidation - The oxidative damage to lipids in samples was measured by the formation of a thiobarbituric acid reactive species (TBARS) during an acid-heating reaction. TBARS were determined by absorbance in a spectrophotometer at 532 nm and expressed as nmol TBARS/mg of protein (Draper and Hadley, 1990).

b) Protein oxidative damage - Protein carbonyl formation was used as an indicator of oxidative damage. Briefly, trichloroacetic acid (20%) was added to protein precipitation for 5 min under 4 °C and centrifuged at 4000 g for 5 min. The proteins were dissolved in 100 μL of sodium hydroxide (NaOH) (200 mM). 100 μL of hydrochloric acid (HCl-2M) or 100 μL of DNPH tubes (10 mM) were added for carbonyl group derivatization. Proteins were washed three times with 1:1 of ethanol: ethyl acetate to remove the excess of DNPH. Samples were dissolved in urea (8 M) pH 2.3, and the formation of the carbonyl level was determined by absorbance in a spectrophotometer at 370 nm (Levine et al., 1990).

c) Sulfhydryl (-SH) content - Oxidative alterations in –SH groups were used to measure the levels of these groups in specific brain regions. Briefly, a 60 μg aliquot sample was diluted in phosphate-buffered saline 10 mM (PBS) and 5,5′-dithionitrobis 2-nitrobenzoic acid (DTNB) was added to the reaction. The result was read at 412 nm in a spectrophotometer after 60 min incubation (Ellman, 1959).

2.9. Indirect ELISA

Pro-inflammatory cytokines TNF-α and IL-1β were quantified in rat serum. The samples were incubated in ELISA plates for 24 h. The plates were then washed three times with Tris-Tween saline (TTBS, 100 mM Tris-HCl, pH 7.5, containing 0.9% NaCl and 0.1% Tween-20). Antibodies were incubated (1: 1000) for 24 h at 4 °C with a gentle shaker. The plates were washed and incubated with anti-rabbit, IgG, linked to peroxidase (1:1000) for 2 h. After washing, a substrate solution (TMB ELISA spectrophotometric detection kit) was added to each well and incubated for 15 min. Sulfuric acid (12 M) was used as a stop solution. ELISA was read at 450 nm in a spectrophotometer.

2.10. Analytical procedures

The coal ash samples were purchased from a thermoelectric plant located in Latin America, Tractebel Suez, State of Santa Catarina, Brazil, and their chemical composition detailed (Silva et al., 2010). The incineration temperature in the combustion chamber was ca. 1000–1500 °C, and about 97.5% of the coal fly ash was captured in the electrostatic precipitators. The chemical composition of utilized coal is detailed in (Silva et al., 2010).

2.11. High-resolution microscopy analysis

Samples for advanced microscopy were prepared by ultrasonication. The samples were characterized using Focused Ion Beam (FIB). FIB is a technique used to evaluate nano-compound assemblages with high resolution-transmission electron microscopy. A FIB setup is a scientific instrument that resembles a scanning electron microscope (SEM), (FIB-SEM). The samples were prepared by a critical point dryer on a glass plate, which was mounted on a SEM stub as describe by Oliveira et al., 2018) (Oliveira et al., 2018).

To provide information on the particles present at the surface, the Dual Beam Focused Ion Beam (FIB) generated by FEI DualBeam™ Helios 600 Nanolab™ was performed. A high-resolution Field Emission Gun (FEG) for SEM; multiple electron detectors for image acquisition, such as through-the-lens detector (TLD), an Everhart-Thornley detector (ETD), a backscattered electron detector (BSED) for compositional information, and a high-resolution focused ion (Ga^+) beam to precisely select, with a spatial resolution of about 10 nm were used.

2.12. Immunofluorescence microscopy

Five slices per hippocampus were obtained using a cryostat at -20 °C (Jung Histoslide, 2000R; Leica; Heidelberg, Germany). The tissue sections were incubated in 5% albumin for 2 h, then incubated with antibodies for 48 h at 4 °C. Anti-GFAP (1:1000) Cell Signaling Technology®. Iba-1 (1:500) FUJIFILM Wako Pure Chemical. After washing, tissue sections were incubated with secondary antibodies, anti-mouse 555 and anti-rabbit 488 from Cell Signaling Technology®, (antibody concentration 1:500). After incubation in secondary antibodies for 1 h and DAPI for 5 min (D9542, MERCK) at room temperature (21 ± 3 °C), the sections were washed several times and submitted to microcopy. The images were acquired using a Microscopy EVOS® FL Auto Imaging System (AMAFD1000 - Thermo Fisher Scientific). The mean was calculated using five slices from each region per animal. Six animals per group were used in the statistical analysis.

2.13. Statistical analysis

Statistical analysis was performed using GraphPad Prism version 7 (GraphPad Software Inc., CA, USA). Data were evaluated by Two-way ANOVA followed by Tukey's multiple comparisons test. The results were expressed as mean ± standard error (S.E.M.). Differences were considered significant when $p < 0.05$ (Callegari-Jacques, 2003).

3. Results

3.1. Weight, glycemia, microglia and astrocyte reactivity

The high-fat diet resulted in a significant increase in animal weight (Supplementary Fig. 2A). Those animals that presented alterations in weight also had altered glycemia levels (Supplementary Fig. 2B). The animals treated with coal ash had no changes in weight and glycemia. Supplementary Figs. 2A and B shows only groups with statistical differences (control versus HFD).

Immunofluorescence was carried out on the hippocampus to evaluate the microglia (iba-1) and astrocyte (GFAP) reactivity (Supplementary Figs. 2C–F). However, the treatments with HFD or coal ash inhalation were found to have no effects on these cells. In Supplementary Fig. 2, only control and HFD groups were showed as representative since other treatments were not able to induce alterations in evaluated parameters.

3.2. High-fat diet associated with coal ash inhalation alters enzymatic activities

The enzymatic activities of SOD, CAT, and GPx in the different

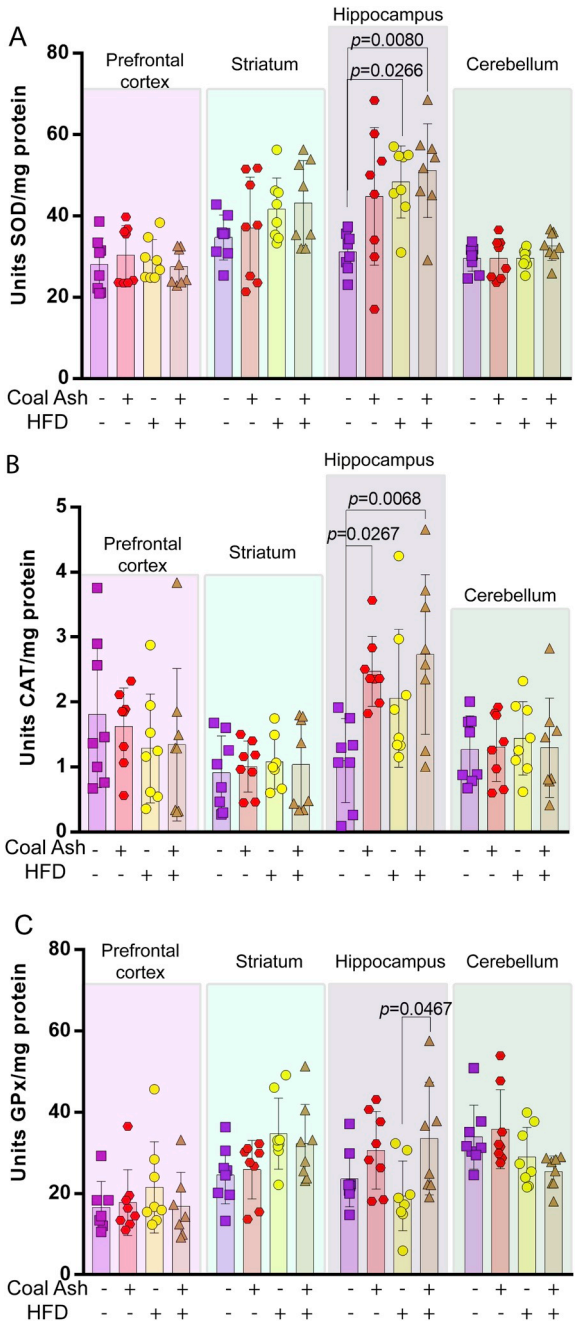

Fig. 2. Quantification of SOD, CAT and GPX enzyme activity in prefrontal cortex, striatum, hippocampus, and cerebellum. High Fat Diet (HFD). The results were expressed as a mean ± standard error (S.E.M.). Data were evaluated by Two-way ANOVA followed by Tukey's multiple comparisons test. $n = 8$ per group. The symbol (−) indicates the absence of treatment, the symbol (+) indicates the presence of treatment.

regions of the brain were investigated in this study. The group that received HFD-associated with coal ash inhalation showed an increase of SOD (Fig. 2A) and CAT (Fig. 2B) activity in the hippocampus over the control group. Obese animals, without coal ash inhalation, showed an increase in SOD activity. Animals with coal ash inhalation showed an increase in CAT activity in the hippocampus.

GPx activity (Fig. 2C) increased only between the HFD and HFD-associated coal ash inhalation. Other brain regions and groups showed no alteration in these enzymes.

3.3. HFD-associated with coal ash inhalation induces oxidative damage

Lipid peroxidation, protein carbonylation and the reduction of disulfide groups as well as GST activity were investigated as parameters of oxidative damage.

In the hippocampus, those animals that received HFD and coal ash inhalation showed high levels of TBARS (Fig. 3A) and carbonylation of protein (Fig. 3B). On the other hand, thiol groups (-SH) decreased in this group (Fig. 3C), complementing the result shown on the carbonylation protein profile.

In the prefrontal cortex, there were alterations between groups that received only coal ash inhalation and HFD-associated with coal ash inhalation, indicating that the obesity associated with coal ash exposure may induce aggravation of lipid damage in the prefrontal cortex. However, in this region, those animals treated with HFD had a reduction of thiols groups.

In the cerebellum, the HFD caused increases in TBARS levels (Fig. 3A), while in the striatum, there was a decrease in –SH induced by treatment association (Fig. 3C). Both striatum and hippocampus had significant reductions of –SH in the HFD + coal ash inhalation group. This reduction in thiol groups may be associated with the proximity of telencephalon and diencephalon.

GST (Fig. 3D) has an essential role in catalyzing the conjugation of reduced glutathione to a substrate, resulting in detoxification. The HFD group, coal ash group and HFD-associated to coal ash inhalation group all showed an increase in GST activity in comparison to the control group.

3.4. Pro-inflammatory cytokines

The pro-inflammatory cytokines, TNF-α and IL-1β were investigated in serum. The animals receiving coal ash inhalation showed increases in IL-1β (Table 1). The group treated only with HFD showed increases in both these cytokines, and the group receiving HFD-associated with coal ash inhalation, had even higher levels of cytokines in the bloodstream.

3.5. High-resolution microscopy

FIB-SEM combines imaging with sectioning. It gives high-resolution images of elements present in coal ash samples by a low voltage scanning electron microscopy. This combination with nano-sectioning becomes a unique tool in the analysis of coal samples. This tool is especially important in understanding the internal wall structure of CCRs and the relationship between elements. Various coal ash components were identified, amongst which pyrite, carbon nanotubes, and Nano magnetite were present in large quantities (Fig. 4).

4. Discussion

The rat chronic obesogenic diet (six months) containing 60% fat used for this investigation resulted in a 40% weight gain. The chronicity of this model allows for the increase of fatty tissue, the changes in biochemical parameters, and very especially, the development of insulin resistance and increasing blood glucose levels. Obese rats showed a glycemia index 20% higher than non-obese rats.

Aspects of vocalization, response to management, appetite, appearance of teeth, fur, eyes, tail, ears and paws were observed weekly as basic health indicators. Only obese animals showed less care with personal hygiene, especially after being exposed to the coal ash inhalation chamber. These results were expected, since the increase in body mass of obese animals, greatly exacerbates hygiene difficulties. The remaining parameters observed, presented healthy characteristics in all animals and there was no mortality due to the models.

Obese rats had high levels of bloodstream cytokines, TNF-α and IL-1β. A constant inflammatory stimulus accompanies the exacerbated expansion of adipose tissue. Obesity is therefore considered to have

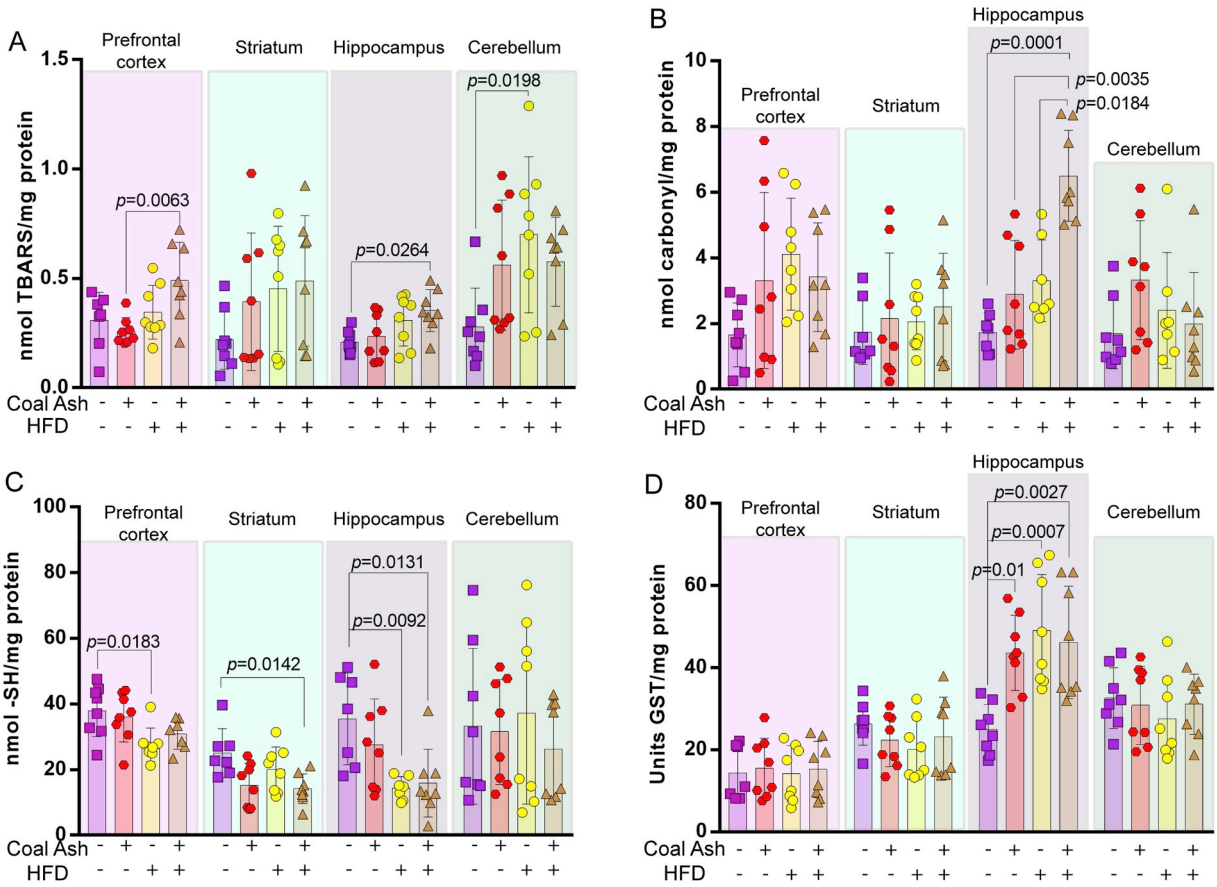

Fig. 3. Oxidative damage in the prefrontal cortex, striatum, hippocampus, and cerebellum. A) TBARS, B) Carbonyl, C) -SH content and D) GST activity. The results were expressed as a mean ± standard error (S.E.M.). Data were evaluated by Two-way ANOVA followed by Tukey's multiple comparisons test. *p* values are embedded in the figure. The symbol (−) indicates the absence of treatment, the symbol (+) indicates the presence of treatment.

inflammatory processes occurring at high levels full time (Reilly and Saltiel, 2017). This tissue releases hormones and harmful molecules, all of which induce endocrine, paracrine and autocrine signaling in various cells throughout the body (Berntsen et al., 2018). The signaling between cells results in the generation of reactive oxygen species and pro-inflammatory cytokines (Bortolin et al., 2018; Rashid et al., 2013).

In obese people, the antioxidant and anti-inflammatory defenses cannot maintain homeostasis. Consequently, increases in ROS and pro-inflammatory cytokines occur which cause damage to lipids and proteins in many organs (Manna and Jain, 2015). In this present study, using the animal model, four structures were investigated: cortex prefrontal, striatum, hippocampus, and cerebellum. The Hippocampus was the region most affected by obesity, showing alterations in enzymatic activity and a decrease in thiol groups.

Due to the inflammatory response induced by obesity, the exposure to xenobiotics may elevate the oxidative stress and inflammation even further (de Bont et al., 2019; Hoseinzadeh et al., 2018; Tongesayi et al., 2013). In this study, the inhalation of coal ash was introduced in obese animals to investigate the effects of environmental contamination in the brains of obese and non-obese rats.

During every breath of air, nanoparticles invade the airways silently and invisibly. The polluted air reaches the lungs and nanoparticles may enter the bloodstream and be distributed to many organs (Krawczynska et al., 2015; Sutto, 2018; Valdiglesias et al., 2013). In our experimental model, the inhalation of coal ash alone can induce an increase of cytokine IL-1β, GST and CAT activity in non-obese rats. However, when the obese rats were exposed to coal ash inhalation, there were significative increases in enzymatic activity as well as damage to lipid and protein carbonylation, unseen excepting in the combination of the two treatments.

All groups of this study increased GST activity. This enzyme assists the metabolization of toxic compounds, and its catalytic reactions transform xenobiotic compounds into soluble products, hence decreasing or inhibiting the cytotoxicity of various compounds (Hayes et al., 2005).

The coal ash particles have many components that can generate toxicity, such as pyrite and carbon nanotubes (Fig. 4A and B). In the presence of water and oxygen, these generate reactive species of oxygen and sulfuric acid and release potential hazardous elements present in their structure, such as mercury, lead, and arsenic. Another component

Table 1
Pro-inflammatory cytokine levels in serum. Indirect ELISA was performed to investigate TNF-α and IL-1β. High Fat Diet (HFD). The results were expressed as a mean ± standard error (S.E.M.). Data were evaluated by Two-way ANOVA followed by Tukey's multiple comparisons test. $n = 8$ per group. * denotes difference to Control $p < 0.01$. ** denotes difference to control $p < 0.001$. # denotes difference to HFD, $p < 0.002$.

	Control	Coal ash	HFD	HFD + Coal ash
TNF-α	11.5 ± 1.4	14.2 ± 1.6	15.33 ± 3.5*	19.84 ± 2.1 **#
IL-1β	113.8 ± 18.83	200.9 ± 45.5*	156.1 ± 12.5**	235.8 ± 45.5**#

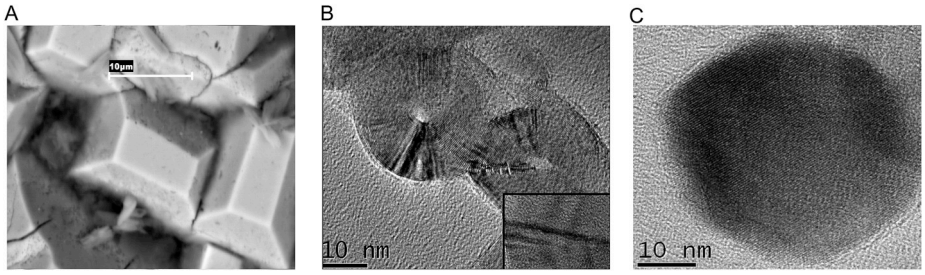

Fig. 4. High-resolution microscopy. FIB-SEM technology allows to define the chemical composition and the structural state of mineral inclusions in coal ash at the ultrafine/nanoscale. A) Pyrite, B) carbon nanotubes and C) Nanomagnetite.

of coal ash is the Nano magnetite (Fig. 4C) which can enter the brain through the olfactory nerve, targeting brain tissue and resulting in ROS production. A postmortem study of 37 subjects living in a metropolis showed Nano magnetite particles in the brain (frontal lobes), the same Nano magnetite particles as are produced by combustion in industrial processes and released into the air (Maher et al., 2016). These nanoparticles bioaccumulate in different regions of the brain, which may be the main factor for neurodegeneration.

As well as these, other potentially harmful elements such as Arsenic, Caesium, Chromium, Iron, Lead, Mercury, sulfide and nanoparticle aggregates are also present in coal ash samples and play a pivotal role in their xenobiotic effects (Li et al., 2013; Oliveira et al., 2018). Our experimental model results emphasize that exposure to these particles leads to significant adverse effects on animal health. It should be noted that exposure to these particles may also have similar implications for human health, and as such, the association between obesity and environmental exposure may be a harmful combination.

The reactivity of astrocytes and microglia was investigated in the hippocampus (Supplementary Fig. 2). Both cells became reactive in the presence of pro-inflammatory stimuli, releasing into bloodstream, high levels of TNF-α and IL-1β. However, HFD, coal ash inhalation, and the associated treatments did not change the reactivity (based on morphology) nor the total number of these cells. Probably, the oxidative damage found in our study, mainly in the rat hippocampus, was the result of reactive oxygen species and the glycation process induced by high levels of blood glucose. The high levels of circulating cytokines may be the result of adipocyte and lung cells stress. Further studies will be necessary to better understand these effects.

5. Conclusion

Here we identify the neurotoxic effects of obesity and coal ash inhalation in an animal model. From the moment that nanoparticles enter the brain, bioaccumulation occurs, and oxidative damage results. Since the hippocampus is affected directly by hyperglycemia and because there already is an underlying pro-inflammatory stimulation generated by excess adipose tissue, the interaction of these nanoparticles from polluted air, can cause increased chronic damage, resulting in neurodegenerative diseases.

Data availability

The data that support the findings of this study are available from the corresponding author upon reasonable request.

Conflicts of interest

The authors declare no competing financial interests.

Acknowledgments

FAPERGS/CNPq12/2014-PRONEX 16/2551–0000 499-4, CAPES, CNPq and UFRGS. We also thank the collaboration of the DE LA COSTA university (Colombia).

Appendix A. Supplementary data

Supplementary data to this article can be found online at https://doi.org/10.1016/j.fct.2019.110766.

References

HEI, 2019. Health Effects Institute. State of Global Air. Special Report. Health Effects Institute, Boston, MA Avaiable in. https://www.stateofglobalair.org/sites/default/files/soga_2019_report.pdf.

Aebi, H., 1984. Catalase in vitro. Methods Enzymol. 105, 121–126.

Alford, S., Patel, D., Perakakis, N., Mantzoros, C.S., 2018. Obesity as a risk factor for Alzheimer's disease: weighing the evidence. Obes. Rev. 19 (2), 269–280. https://doi.org/10.1111/obr.12629.

Alvarez-Pedrerol, M., Rivas, I., Lopez-Vicente, M., Suades-Gonzalez, E., Donaire-Gonzalez, D., Cirach, M., ... Sunyer, J., 2017. Impact of commuting exposure to traffic-related air pollution on cognitive development in children walking to school. Environ. Pollut. 231 (Pt 1), 837–844. https://doi.org/10.1016/j.envpol.2017.08.075.

Animals, Guide, 2011. Guide for the Care and Use of Laboratory Animals. avaiable in: https://www.ncbi.nlm.nih.gov/books/NBK54050/pdf/Bookshelf_ NBK54050.pdf.

Berntsen, H.F., Bolling, A.K., Bjorklund, C.G., Zimmer, K., Ropstad, E., Zienolddiny, S., ... Bodin, J., 2018. Decreased macrophage phagocytic function due to xenobiotic exposures in vitro, difference in sensitivity between various macrophage models. Food Chem. Toxicol. 112, 86–96. https://doi.org/10.1016/j.fct.2017.12.024.

Bluher, M., 2019. Obesity: global epidemiology and pathogenesis. Nat. Rev. Endocrinol. https://doi.org/10.1038/s41574-019-0176-8.

Bortolin, R.C., Vargas, A.R., Gasparotto, J., Chaves, P.R., Schnorr, C.E., Martinello, K.B., ... Moreira, J.C.F., 2018. A new animal diet based on human Western diet is a robust diet-induced obesity model: comparison to high-fat and cafeteria diets in term of metabolic and gut microbiota disruption. Int. J. Obes. 42 (3), 525–534. https://doi.org/10.1038/ijo.2017.225.

Bradford, M.M., 1976. A rapid and sensitive method for the quantitation of microgram quantities of protein utilizing the principle of protein-dye binding. Anal. Biochem. 72, 248–254.

Callegari-Jacques, S., 2003. *Bioestatística princípios e aplicações*. Artmed. Porto Alegre/BRAZIL.

de Assis, A.M., Rieger, D.K., Longoni, A., Battu, C., Raymundi, S., da Rocha, R.F., Perry, M.L., 2009. High fat and highly thermolyzed fat diets promote insulin resistance and increase DNA damage in rats. Exp. Biol. Med. 234 (11), 1296–1304. https://doi.org/10.3181/0904-rm-126.

de Bont, J., Casas, M., Barrera-Gomez, J., Cirach, M., Rivas, I., Valvi, D., ... Vrijheid, M., 2019. Ambient air pollution and overweight and obesity in school-aged children in Barcelona, Spain. Environ. Int. 125, 58–64. https://doi.org/10.1016/j.envint.2019.01.048.

Draper, H.H., Hadley, M., 1990. Malondialdehyde determination as index of lipid peroxidation. Methods Enzymol. 186, 421–431.

Ellman, G.L., 1959. Tissue sulfhydryl groups. Arch. Biochem. Biophys. 82 (1), 70–77.

Gasparotto, J., Chaves, P.R., da Boit Martinello, K., da Rosa-Siva, H.T., Bortolin, R.C., Silva, L.F.O., ... Moreira, J.C.F., 2018. Obese rats are more vulnerable to inflammation, genotoxicity and oxidative stress induced by coal dust inhalation than non-obese rats. Ecotoxicol. Environ. Saf. 165, 44–51. https://doi.org/10.1016/j.ecoenv.2018.08.097.

Habig, W.H., Pabst, M.J., Jakoby, W.B., 1974. Glutathione S-transferases. The first enzymatic step in mercapturic acid formation. J. Biol. Chem. 249 (22), 7130–7139.

Hayes, J.D., Flanagan, J.U., Jowsey, I.R., 2005. Glutathione transferases. Annu. Rev. Pharmacol. Toxicol. 45, 51–88. https://doi.org/10.1146/annurev.pharmtox.45.120403.095857.

Hoseinzadeh, E., Taha, P., Wei, C., Godini, H., Ashraf, G.M., Taghavi, M., Miri, M., 2018. The impact of air pollutants, UV exposure and geographic location on vitamin D deficiency. Food Chem. Toxicol. 113, 241–254. https://doi.org/10.1016/j.fct.2018.01.052.

Krawczynska, A., Dziendzikowska, K., Gromadzka-Ostrowska, J., Lankoff, A., Herman,

A.P., Oczkowski, M., ... Kruszewski, M., 2015. Silver and titanium dioxide nanoparticles alter oxidative/inflammatory response and renin-angiotensin system in brain. Food Chem. Toxicol. 85, 96–105. https://doi.org/10.1016/j.fct.2015.08.005.

Levine, R.L., Garland, D., Oliver, C.N., Amici, A., Climent, I., Lenz, A.G., ... Stadtman, E.R., 1990. Determination of carbonyl content in oxidatively modified proteins. Methods Enzymol. 186, 464–478.

Li, Q., Hu, X., Bai, Y., Alattar, M., Ma, D., Cao, Y., ... Jiang, C., 2013. The oxidative damage and inflammatory response induced by lead sulfide nanoparticles in rat lung. Food Chem. Toxicol. 60, 213–217. https://doi.org/10.1016/j.fct.2013.07.046.

Maher, B.A., Ahmed, I.A., Karloukovski, V., MacLaren, D.A., Foulds, P.G., Allsop, D., ... Calderon-Garciduenas, L., 2016. Magnetite pollution nanoparticles in the human brain. Proc. Natl. Acad. Sci. U. S. A. 113 (39), 10797–10801. https://doi.org/10.1073/pnas.1605941113.

Manna, P., Jain, S.K., 2015. Obesity, oxidative stress, adipose tissue dysfunction, and the associated health risks: causes and therapeutic strategies. Metab. Syndrome Relat. Disord. 13 (10), 423–444. https://doi.org/10.1089/met.2015.0095.

McCormack, M.C., Belli, A.J., Kaji, D.A., Matsui, E.C., Brigham, E.P., Peng, R.D., Hansel, N.N., 2015. Obesity as a susceptibility factor to indoor particulate matter health effects in COPD. Eur. Respir. J. 45 (5), 1248–1257. https://doi.org/10.1183/09031936.00081414.

Misra, H.P., Fridovich, I., 1972. The role of superoxide anion in the autoxidation of epinephrine and a simple assay for superoxide dismutase. J. Biol. Chem. 247 (10), 3170–3175.

Oliveira, M.L., Da Boit, K., Schneider, I.L., Teixeira, E.l.C., Crissien Borrero, T.J., Silva, L.F., 2018. Study of coal cleaning rejects by FIB and sample preparation for HR-TEM: mineral surface chemistry and nanoparticle-aggregation control for health studies. J. Clean. Prod. 188, 662–669.

Paxinos, G., Watson, C., 2007. The Rat Brain in Stereotaxic Coordinates, sixth ed. Elsevier.

Rashid, K., Sinha, K., Sil, P.C., 2013. An update on oxidative stress-mediated organ pathophysiology. Food Chem. Toxicol. 62, 584–600. https://doi.org/10.1016/j.fct.2013.09.026.

Reilly, S.M., Saltiel, A.R., 2017. Adapting to obesity with adipose tissue inflammation. Nat. Rev. Endocrinol. 13 (11), 633–643. https://doi.org/10.1038/nrendo.2017.90.

Rovira, J., Schuhmacher, M., Nadal, M., Domingo, J.L., 2019. Contamination by coal dust in the neighborhood of the tarragona harbor (catalonia, Spain): a preliminary study. Open Atmos. Sci. J. 12, 14–20. https://doi.org/10.2174/1874282301812010014.

Siino, V., Amato, A., Di Salvo, F., Caldara, G.F., Filogamo, M., James, P., Vasto, S., 2018. Impact of diet-induced obesity on the mouse brain phosphoproteome. J. Nutr. Biochem. 58, 102–109. https://doi.org/10.1016/j.jnutbio.2018.04.015.

Silva, L.F.O., Ward, C.R., Hower, J.C., Izquierdo, M., Waanders, F., Querol, X., 2010. Mineralogy and Leaching Characteristics of Coal Ash from a Major Brazilian Power Plant. *Coal Combustion And Gasification Products*.

Sutto, T.E., 2018. Magnetite fine particle and nanoparticle environmental contamination from industrial uses of coal. Environ. Pollut. 243 (Pt A), 528–533. https://doi.org/10.1016/j.envpol.2018.08.080.

Tongesayi, T., Fedick, P., Lechner, L., Brock, C., Le Beau, A., Bray, C., 2013. Daily bioaccessible levels of selected essential but toxic heavy metals from the consumption of non-dietary food sources. Food Chem. Toxicol. 62, 142–147. https://doi.org/10.1016/j.fct.2013.08.052.

Valdiglesias, V., Costa, C., Kilic, G., Costa, S., Pasaro, E., Laffon, B., Teixeira, J.P., 2013. Neuronal cytotoxicity and genotoxicity induced by zinc oxide nanoparticles. Environ. Int. 55, 92–100. https://doi.org/10.1016/j. envint .2013.02.013.

Wendel, A., 1981. Glutathione peroxidase. Methods Enzymol. 77, 325–333.

WHO, 2018. Global Ambient Air Quality Database (Update 2018). 2019-01-22 12:36:50 WHO Avaiable in: https://www.who.int/airpollution/data/cities/en/.

Xue, J., Ideraabdullah, F.Y., 2016. An assessment of molecular pathways of obesity susceptible to nutrient, toxicant and genetically induced epigenetic perturbation. J. Nutr. Biochem. 30, 1–13. https://doi.org/10.1016/j.jnutbio .2015.09.002.